Building and Environment 47 (2012) 243–255

Contents lists available at ScienceDirect

Building and Environment

journal homepage: www.elsevier.com/locate/buildenv

A new zero-equation turbulence model for micro-scale climate simulation

Cheng Li, Xiaofeng Li*, Yaxuan Su, Yingxin Zhu

Department of Building Science, School of Architecture, Tsinghua University, Beijing 100084, China

ARTICLE INFO

Article history:
Received 22 April 2011
Received in revised form
13 July 2011
Accepted 14 July 2011

Keywords:
Micro-scale climate
Turbulence model
Zero-equation turbulence model
Computational wind engineering

ABSTRACT

Micro-scale climate is vital for the health and comfort of residents in urban areas. Simulation platforms being used to predict micro-scale climate usually take CFD (Computational Fluid Dynamics) as their core procedure. The popular turbulence models in practical CFD application for micro-scale climate are the k-ε series models. Given that the two-equation models might cost too much CPU time, they can hardly be applied at the design stage of complex urban area. Compared with the two-equation models, zero-equation turbulence models can reduce the computer load significantly. This paper proposes a new two-layer zero-equation turbulence model specific for the micro-scale climate simulations. The model assumes the turbulence viscosity as a function of velocity deformation rate and the length scale in the inner layer and function of length scale and local mean velocity in the outer layer. Validated with the wind-tunnel experiment data, this new zero-equation turbulence model can give reasonably acceptable results in micro-scale climate simulations. Besides, it costs much less CPU time and computer memory than the standard k-ε model does. This new zero-equation turbulence model can be an applicable alternative in micro-scale climate research.

© 2011 Elsevier Ltd. All rights reserved.

1. Introduction

The micro-scale climate in built-up urban areas is important to the health and comfort of human beings [1]. Additionally, it significantly affects the energy consumption and the natural ventilation of buildings within the area. Therefore designing and optimizing the micro-scale climate in the neighborhood of buildings is a highly concerned issue at the stage of urban or residential area design [2–6]. A simulation platform supporting designers to predict the micro-scale climate can efficiently improve the quality of sustainable design. Thus some cost-effective simulation platforms have huge potential in assisting the design process in practice.

The micro-scale climate is an interaction of various physical parameters, which include the airflow velocity, air temperature, solar radiation intensity, pollutant concentration and so on. Given this circumstance, the simulation of micro-scale climate usually needs a coupled simulation platform in which multiple physical parameters could be analyzed simultaneously [7]. Such kind of platform generallytakes CFD (Computational Fluid Dynamics) as its core procedure. In CFD the turbulence model of airflow simulation is critical to the accuracy of simulation and usually is the main factor that consumes the computer resource and reduces the efficiency of simulation [8]. So far turbulence models being widely used are Direct Numerical Simulation (DNS), Large Eddy Simulation (LES) and Reynolds Average Navier-Stocks (RANS). Although having inherent deficiencies in representing the flow pattern in wake regions near buildings, the RANS models (e.g. k–ε and k-l models) can represent the general flow pattern well in urban areas and are still the popular choices in practical applications even if accuracy and cost are compromised to some extent [1,9,10]. Moreover, to improve the performance in wake regions, various modified RANS models (one or two-equation models) have been proposed and applied in recent research on micro-climate [11,12].

The micro-climate platform has to solve the energy balance equation at each surface of buildings within the urban canopy. Hence the CFD simulation has to be coupled with heat conduction simulation at walls or ground. That means the CFD takes the surface temperature from the heat conduction simulation as its boundary condition and the heat conduction simulation uses the air temperature from CFD as an input for further operation [13]. Since computational costs of the heat conduction simulation are usually much less than CFD, increasing the efficiency of CFD is vital for practical application especially when the object of study is much more complicated than a single urban block. From this perspective, a zero-equation turbulence model which can efficiently decrease the simulation load by reducing differential equations to be solved is of great importance for further research on micro-climate. Some research has already been conducted on zero-equation turbulence models. Chen and Xu [14] proposed a zero-equation turbulence

* Corresponding author. Tel.: +86 10 62779993; fax: +86 10 62773461.
E-mail address: xfli@tsinghua.edu.cn (X. Li).

0360-1323/$ – see front matter © 2011 Elsevier Ltd. All rights reserved.
doi:10.1016/j.buildenv.2011.07.015

Table 1
Characteristics of zero-equation turbulence models.

Model.	Applicable flow patterns	Limitations
Mixed-length model	Flow in boundary-layers	Only suitable for boundary-layers;
B-L & C-S model	Channel or pipe flow	Can't handle boundary-layers or separated flow
C-X model	Flow in indoor environment	Doubtable for outdoor environment

model specifically designed for indoor airflow simulation in 1998. Subsequent validation demonstrated by Srebric [15] also showed that the simulation results given by the zero-equation turbulence model can agree considerably well with experiment data. Due to the advantages of this zero-equation turbulence model on accuracy and efficiency, it has been widely used in the application of indoor airflow simulations [16–18].

The expanding physical range of micro-scale climate simulation and increasing computer load are now calling for an efficient turbulence model for the coupled simulation platform for outdoor environment. Considering such situation, this paper will propose a new zero-equation turbulence model for the micro-scale climate simulation in order to improve the simulation efficiency and hopefully it will be used in further coupled simulations.

2. Reviews on zero-equation turbulence models

The k-ε series models and zero-equation turbulence models all belong to eddy viscosity turbulence models. In zero-equation turbulence models, turbulence viscosity is expressed by an algebraic equation without additional differential equations. The research of zero-equation turbulence models dates back to 1925 when Prandtl proposed the mixed-length hypothesis [19] based on the analogy between the molecular transport and the flow lump motions. In mixed-length hypothesis, the turbulence viscosity can be calculated by the following formula:

$$\mu_t = \rho l^2 |d\overline{u}/dy| \tag{1}$$

where μ_t is the eddy viscosity, l represents the mixing length, $\overline{u}$ represents the flow velocity and y is the direction normal to the main flow. Although it is a half-empirical model, in some cases it can obtain quite convincible results.

In 1942, Prandtl proposed a new zero-equation turbulence model suitable for the free shear flows [20], in the form of:

$$\mu_t = \rho C \delta |u_{\max} - u_{\min}| \tag{2}$$

where δ represents the thickness of the shear layer, $u_{\max}$ and $u_{\min}$ are the maximum velocity and the minimum velocity respectively. C is an empirical parameter.

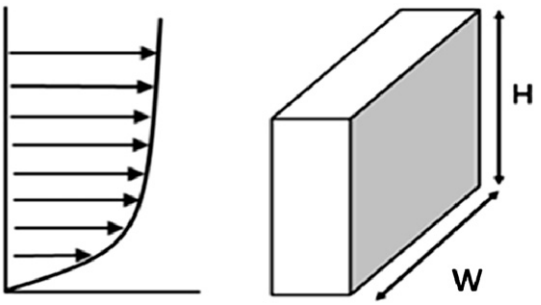

Fig. 1. Normalized width of building.

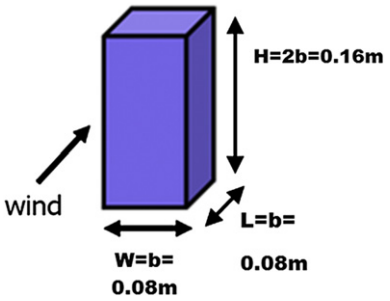

Fig. 2. Schema of the square cuboid in wind-tunnel experiment.

According to the dimensional analysis, the first Prandtl zero-equation turbulence model postulates the turbulence viscosity as the product of the velocity deformation rate scale S (with the unit of s^{-1}) and the square of turbulence length scale l^2 (with the unit of m^2), while the second Prandtl zero-equation turbulence model treats the turbulence viscosity as the product of velocity scale v (with the unit of m/s) and length scale.

Since then many efforts have been made to extend applicability of the zero-equation turbulence models. Smith and Cebeci proposed the Cebeci-Smith model in 1967 [21]. The C-S model is a two-layer zero-equation turbulence model. It treats fluid flow into two sub-layers and gives different forms of turbulence

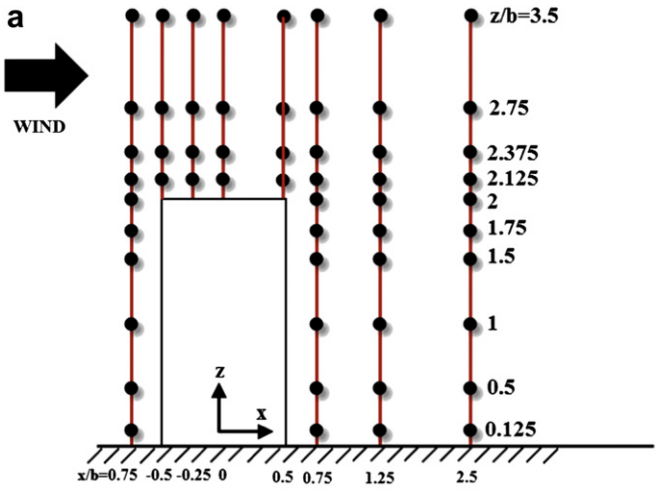

Vertical measuring cross-section at the center of the cuboid (y=0)

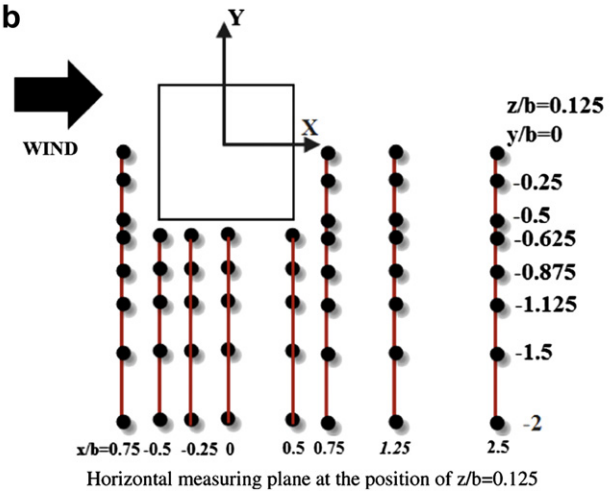

Horizontal measuring plane at the position of z/b=0.125

Fig. 3. Configuration of measuring points.

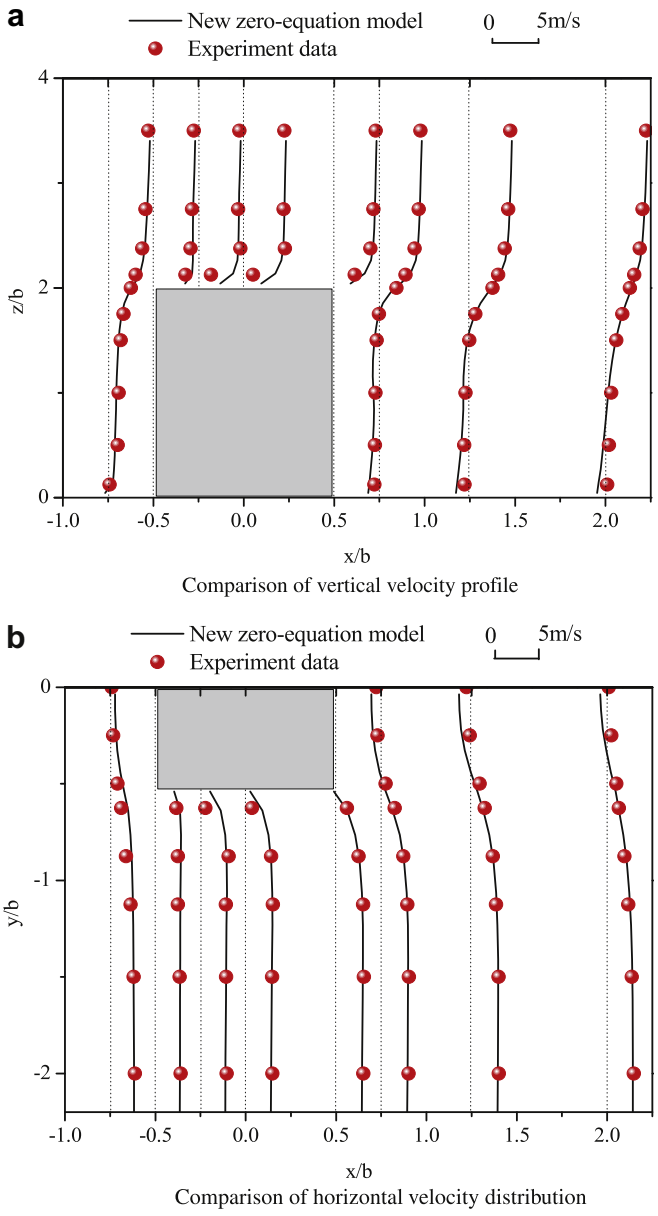

Fig. 4. Comparison between experiment data and simulation results.

viscosity respectively. The C-S model is suitable for the high-speed flows with thin attached boundary-layers but the thickness of the boundary layer should be determined while using it. Later in 1978 Bladwin and Lomax proposed another two-layer model [22] which gives another form of equations in the two layers and is not necessary to judge the boundary-layer edge. Both C-S model and B-L model were popular in the application of engineering field [23]. Although reasonable consistency had been proved in the simulation of channel or pipe flow, the C-S model and B-L model do not perform well in boundary-layer and separated flows, for most of the assumption and empirical constant do not hold in these flows [14,24].

To meet the demand of the airflow simulation in rooms, Chen and Xu proposed a new zero-equation turbulence model (thereafter denoted as C-X model in this paper) in 1998 [14]. It assumes the turbulence viscosity as a function of local mean velocity v and the distance l from the simulation node to the nearest wall:

$$\mu_t = 0.03874\rho v l \tag{3}$$

The constant 0.03874 is an empirical parameter based on the DNS (Direct Numerical Simulation) and experiment measurement of natural convection, forced convection and mixed convection. This model can efficiently and reliably simulate the airflow pattern in the indoor situations. Due to its advantages in indoor air quality design and HVAC application, this model was embedded into the Airpak toolkit in 2001 [25]. However, since the constant 0.03874 is calibrated according to DNS simulation of indoor environment, the reliability of C-X model in outdoor environment is doubtable, so that rare research has applied it for outdoor condition.

Table 1 summarizes the characteristics of all the zero-equation models mentioned above.

In summary, the essences of zero-equation turbulence models are using the specific assumptions and empirical constants to represent the turbulence characteristics of specific kind of flow patterns. Therefore, a new zero-equation model specifically proposed for airflow around buildings is desirable in the future application of micro-scale climate simulation.

3. A new zero-equation turbulence model for outdoor airflow simulation

The purpose of the new zero-equation turbulence model is to achieve the similar accuracy as the two-equation models in airflow simulation around buildings. The new zero-equation turbulence model is proposed according to the analysis of turbulence viscosity distribution obtained by the standard k-ε model. Since the mixed-length model performs well in boundary layers, the new zero-equation model takes the form of mixed-length turbulence model to represent the airflow near buildings. On the other hand, considering the good performance of C-X model in void opening space, the format of C-X model is applied in the new zero-equation model for the area above the urban canopy.

Hence the new zero-equation turbulence model is in the form of two-layers:

$$\mu_t = \max(\mu_{in}, \mu_{out}) \tag{4}$$

In the inner layer, the turbulence viscosity is expressed as a function of velocity deformation rate S (with the unit of s^{-1}) and the square of the length scale l^2 (with the unit of m^2).

$$\mu_{in} = (C_{in} \cdot l)^2 \cdot S \tag{5}$$

where S is the velocity deformation rate:

$$S = \sqrt{0.5\left(\partial u_i/\partial x_j + \partial u_j/\partial x_i\right)^2} \tag{6}$$

l is the distance to the nearest wall or ground. The parameter C_{in} will be discussed later.

In the outer layer, the turbulence viscosity is in the form of:

$$\mu_{out} = C_{out} \cdot V \cdot l \tag{7}$$

where l is still the distance to the nearest wall or ground, V is local mean velocity $\sqrt{u_i u_i}$ and C_{out} is the outer layer parameter.

Since the inner layer model takes charge of the turbulence near the building, it should represent the major characteristics of turbulence induced by buildings. Numerically these characteristics are the scale of turbulence and variation of the eddy viscosity related with different positions. Hence the new zero-equation model proposes a dimensionless parameter C_{in} as the product of φ_{CH} and φ_H to represent these two characteristics respectively:

$$C_{in} = \varphi_{CH}\varphi_H \tag{8}$$

Length of recirculation is usually taken as the length scale of turbulence in the research of micro-climate. Here φ_{CH} integrates the

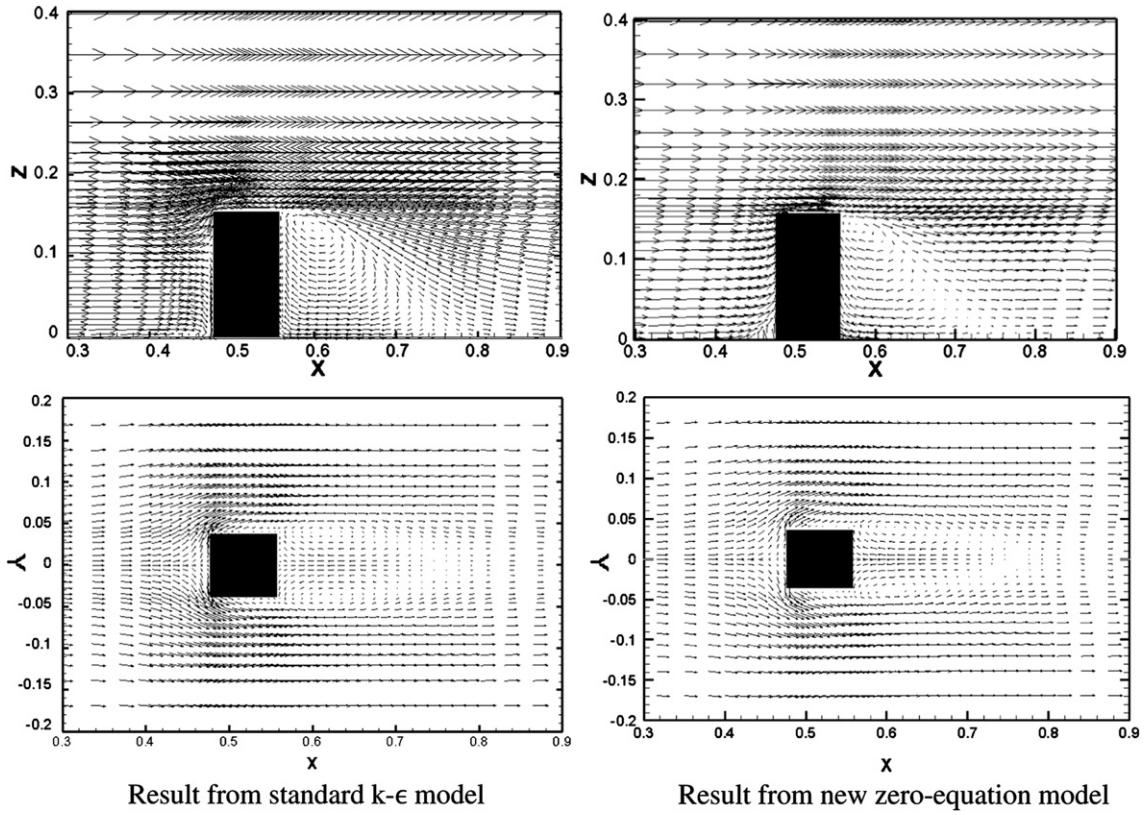

Fig. 5. Vertical profile and cross section of flow pattern at height $z/b = 0.125$.

building's geometry to represent the length scale of turbulence. It can be expressed as Eq. (9) which is settled by regression analysis. The analysis is conducted considering distribution of turbulence viscosity and the length of recirculation behind building gained by simulation of standard k-ε model. Geometry scale in the formula of φ_{CH} is normalized by a characteristic length which is the height of building H in this model:

$$\varphi_{CH} = 1.8\left[1 - \exp\left(-0.645\eta_{CH}^{0.8}\right)\right] \tag{9}$$

where $\eta_{CH} = W/H$ is the normalized width as illustrated in Fig. 1. W, H and L represent the width, height and length of the building respectively.

Besides, according to the distribution of eddy viscosity, the eddy viscosity would vary with the change of vertical position and the height of building. Based on that, the parameter φ_H is expressed as:

$$\varphi_H = \exp[-2\cdot\min(z/H, 1)] \tag{10}$$

In contrast to the inner layer model, the outer layer model is designed to represent the airflow pattern above the buildings. Hence in the situation without any building the outer layer model should be able to represent the flow pattern from the inflow boundary to outlet boundary. Inflow boundary condition usually takes the AIJ's recommendation [9]:

$$u(z) = u_s(z/z_s)^{\alpha} \tag{11}$$

$$\mu = C_\mu k(z)^2/\varepsilon(z) \tag{12}$$

$$k(z) = (I(z)u(z))^2 \tag{13}$$

$$\varepsilon(z) = \alpha C_\mu^{0.5} k(z)(u_s/z_s)(z/z_s)^{\alpha-1} \tag{14}$$

$$I(z) = I_G\cdot(z/z_G)^{-\alpha-0.05} \tag{15}$$

According to the formulation in outer layer, the turbulence viscosity should be:

$$\mu = C_{out}\cdot u\cdot z = C_\mu k(z)^2/\varepsilon(z) \tag{16}$$

Considering Eqs. (11)–(16), the parameter C_{out} is expressed as:

$$C_{out} = C_\mu^{0.5}\cdot I_G^2\cdot Z_G^{2\alpha+0.1}\cdot Z^{0.9-2\alpha}/\alpha \tag{17}$$

where $C_\mu = 0.09$, Z_G is the reference height which in Beijing is 350 m, Z is the height of the node point, $\alpha = 0.22$ is the parameter of ground roughness of Beijing, $I_G = 0.1$ is a constant given by AIJ [9].

4. Validation of the new zero-equation turbulence model

To verify the performance of the new zero-equation turbulence model, a simulation on the airflow around a cuboid is conducted using the new zero-equation model. The results of the simulation are then compared with the wind-tunnel experiment results by Meng and Hibi [26], as AIJ did in their research of CFD prediction of pedestrian wind environment [10].

4.1. Outline of wind-tunnel experiment and CFD simulation

In Meng and Hibi's experiment, airflow around a shape square cuboid whose size ratio is 2:1:1 was measured in a turbulence boundary layer, in which the exponent parameter for the power law of the vertical profile of average wind velocity was 0.27. The shape

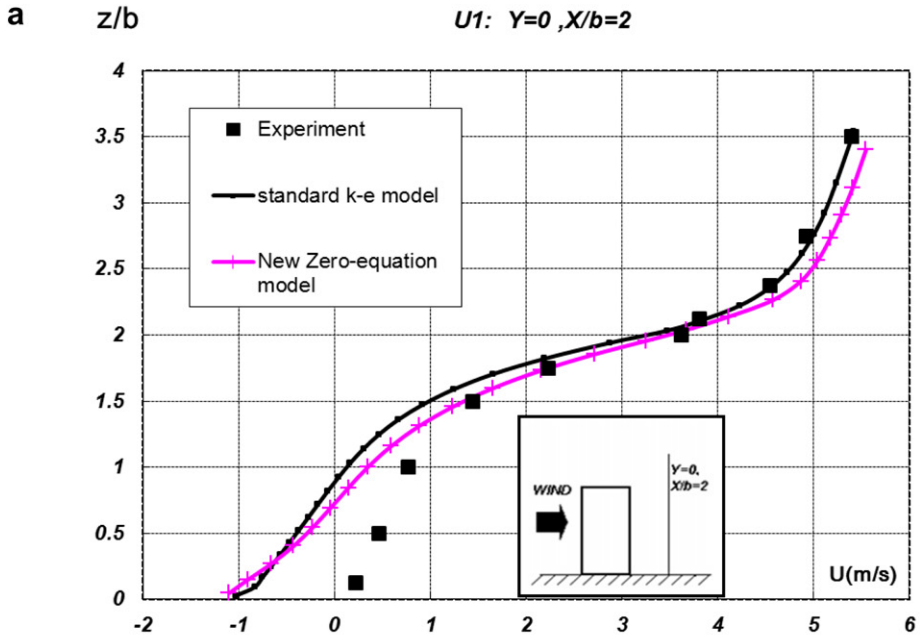

Parallel comparison between standard k-ϵ model and new zero-equation model at the vertical testing line (x/b=2)

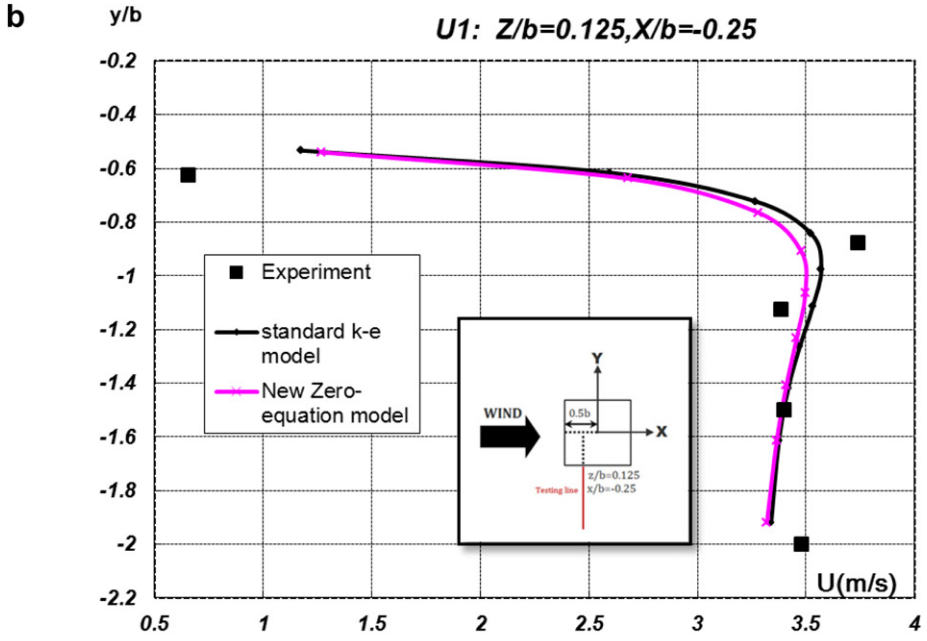

Parallel comparison between standard k-ϵ model and new zero-equation model at the horizontal testing line (z/b=0.125, x/b=-0.25)

Fig. 6. Parallel comparison at testing lines.

size of this cuboid was 0.16 m in height (H) and 0.08 m in width and length (W and L) as shown in Fig. 2.

Velocities are measured and compared on a vertical cross section at the center of the cuboid (Fig. 3(a)) and on a horizontal cross section at the position of $z/b = 0.125$ around the block (Fig. 3(b)). In Fig. 3 the position of the measuring point is represented by sphere on the red line.

All CFD settings used in this simulation are the same as those in AIJ's research except for the turbulence model.

4.2. Validation of the new zero-equation turbulence model

The CFD results calculated by the new zero-equation turbulence model are compared with the wind-tunnel experiment statistics as

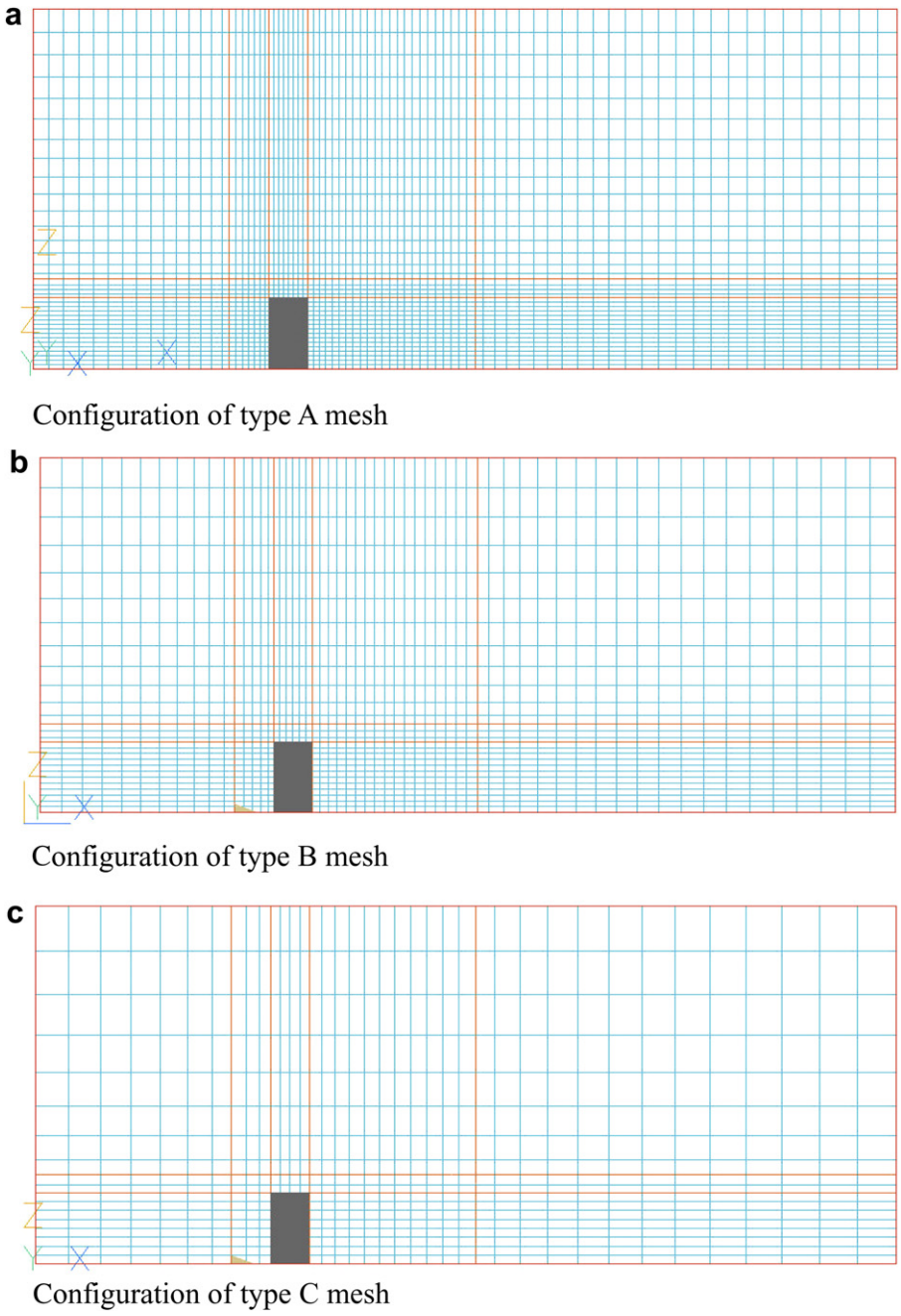

Fig. 7. Mesh configurations for three types.

shown in Fig. 4(a) and Fig. 4(b). The longitudinal dotted lines represent the positions of the measuring line in experiment. Wind velocities are plotted transversely along the lines. Experiment data at testing points are represented by red spheres while simulation results are plotted by black lines. Positive velocities are on the right side of the dotted line and negative are on the left side of the line.

According to the illustrations, the new zero-equation turbulence model shows good performance when being used in the simulation of airflow around the block. Simulation results and experiment data agree relatively well especially behind the cuboid.

Meanwhile, the standard k-ε turbulence model is also applied on the same simulation study. Parallel comparison between the results of standard k-ε model and new zero-equation model are conducted as shown in Fig. 5. According to Fig. 5, flow pattern of zero-equation model and standard k-ε are similar. The reattachment length behind the cuboid in standard k-ε case is 0.2 m, i.e. $X_f = 2.5b$. This phenomenon is similar as reported in previous research [27]. On the other hand, reattachment length behind the cuboid in zero-equation case is 0.19 m, which means the X_f is 2.38b. Conclusion could be drawn from Fig. 5 that the capability of zero-equation model to capture recirculation has similar accuracy as standard k-ε model.

Fig. 6 is a comparison of velocity at specific testing lines. The comparison shows that the new zero-equation turbulence model can give relatively similar result as the standard k-ε turbulence model especially in the lower part of the airflow, the results given by the new zero-equation model are even closer to the experiment data.

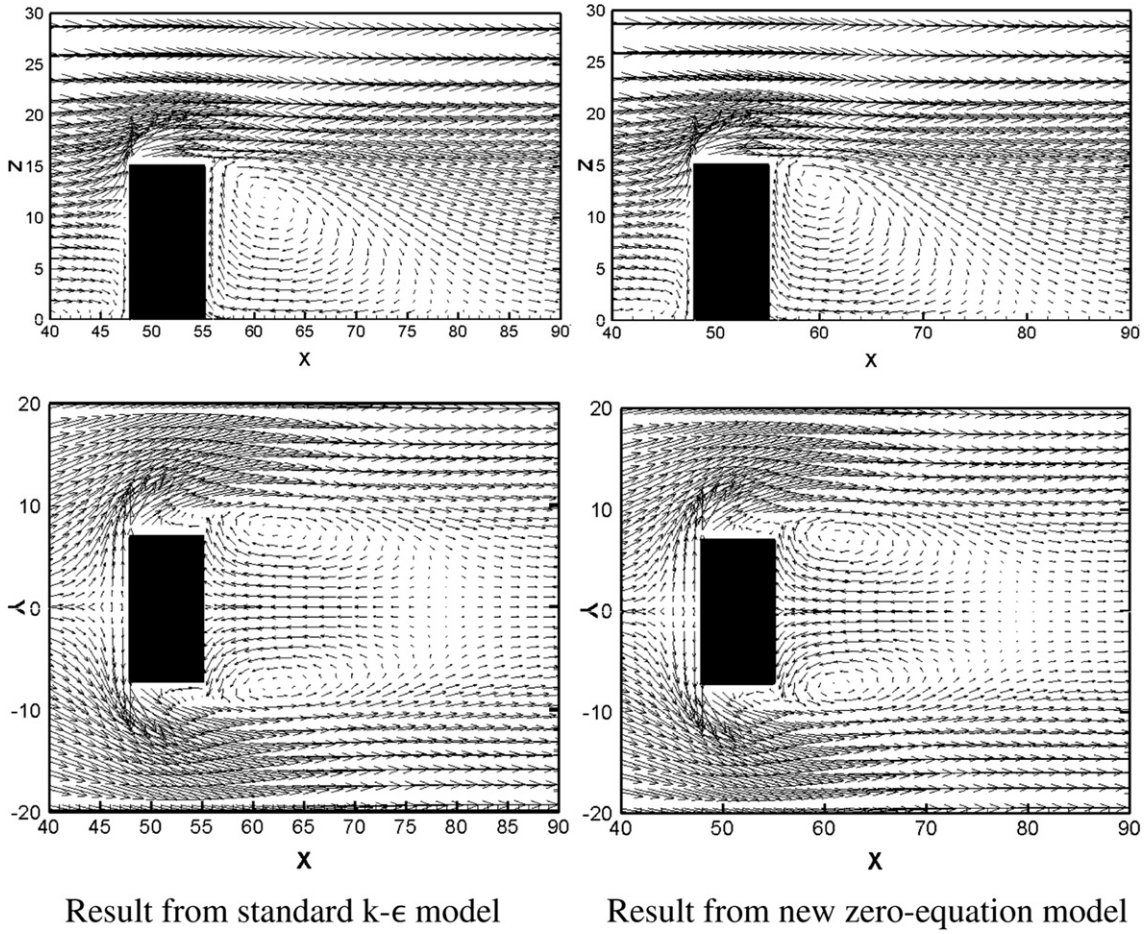

Fig. 8. Vertical profile and horizontal cross section at the height $z = 1.5$ m using type A mesh.

5. Application on single-building simulation

To test the capability of the new zero-equation turbulence model in practical application, a series of simulations are conducted by using both the new zero-equation turbulence model and the standard k-ε model.

5.1. Geometric details

The building's size is 8 m × 16 m × 16 m, thus $\varphi_{CH} = 1$. The whole simulation domain is set to 176 m × 128 m × 80 m. As is recommended in the AIJ's guideline of CFD settings, the blockage ratio (Area of vertical section of the building divided by area of vertical section of the simulation domain) in case is only 1% which is much lower than 3% in the guideline [9]. The distance from the inlet to the building is 48 m, which is 6 times of the building's height. At the y-z cross section the block is located on the middle line.

5.2. Boundary conditions

Inflow boundary conditions for k-ε model:

$$u(z) = u_s(z/z_s)^{\alpha}$$

$$k(z) = (I(z)u(z))^2$$

$$\varepsilon(z) = \alpha C_{\mu}^{0.5} k(z)(u_s/z_s)(z/z_s)^{\alpha-1}$$

$$I(z) = \begin{cases} 0.1\cdot(z_b/z_G)^{-\alpha-0.05} & z \le z_b \\ 0.1\cdot(z/z_G)^{-\alpha-0.05} & z \ge z_b \end{cases} \quad (18)$$

Inflow boundary conditions for zero-equation model:

$$u(z) = u_s(z/z_s)^{\alpha}$$

In equations mentioned above $z_s = 350$ m, $z_G = 350$ m, $z_b = 5$ m,u_s is the velocity at the height of z_s,$u_s = 13$ m/s,$\alpha = 0.22$, $C_\mu = 0.09$. Lateral boundary condition is set to symmetry boundary conditions. Outlet boundary is set to outflow boundary condition.

5.3. Mesh details and numerical settings

Three kinds of mesh are applied in simulation, which are 79 × 33 × 36, 59 × 24 × 27 and 38 × 16 × 18. These three kinds are all non-uniform and structured cells with refined cells near the building. In the later sections, these three kinds of mesh are denoted as type A, type B and type C mesh. Type A and type B follow the instruction of AIJ's mesh settings [9], in which the mesh resolutions are 1/20 and 1/10 of the building scale respectively. The mesh configuration is shown in Fig. 7. The SIMIPLE algorithm and upwind-scheme are applied in the simulation. The Reynolds number based on height of building H and u_s is 1.31×10^7.

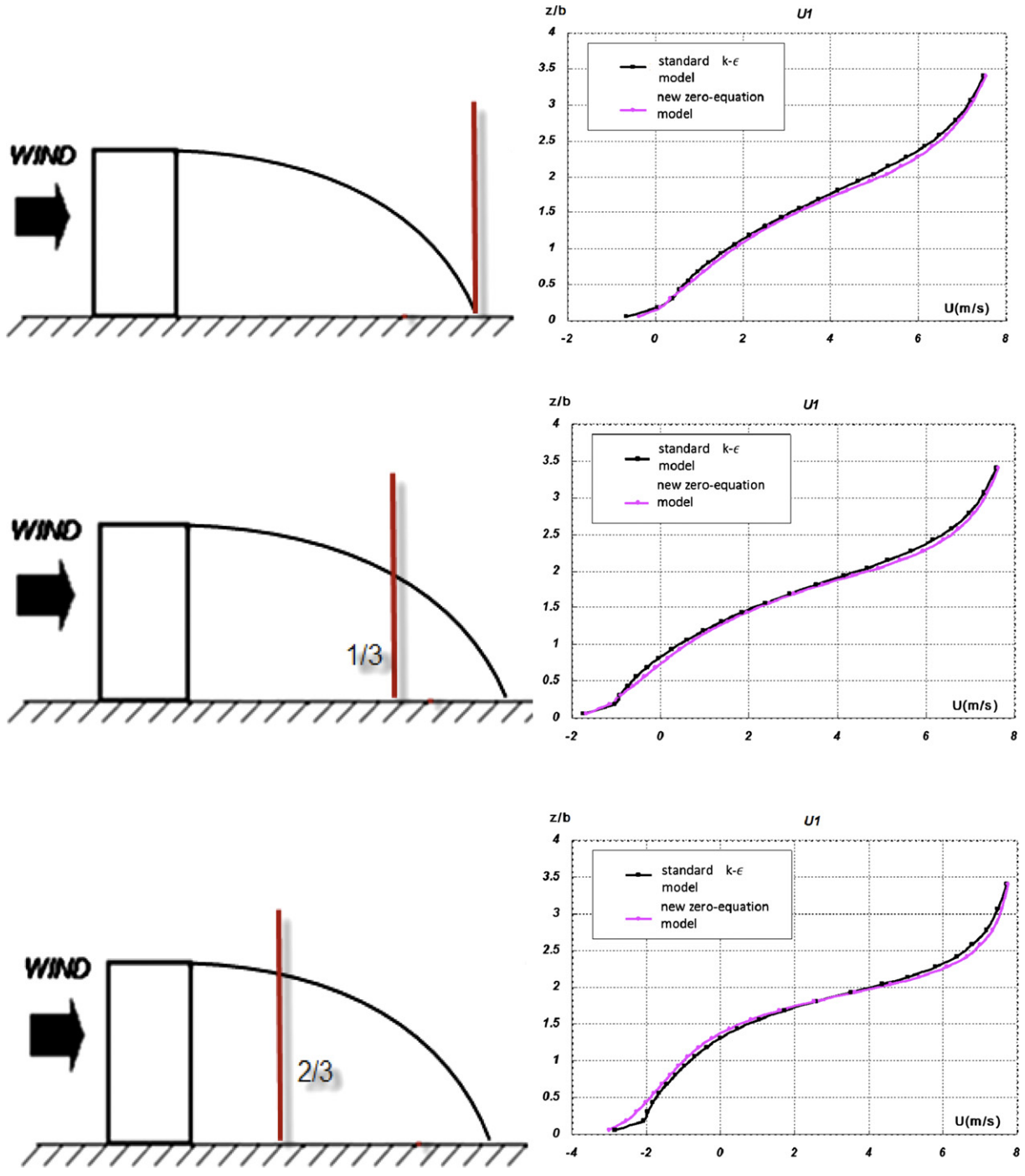

Fig. 9. Vertical profiles at testing point.

5.4. Parallel comparison of the results between the zero-equation turbulence model and standard k-ε model

Fig. 8 shows the vertical profile of the airflow and its horizontal distribution at the height $z = 1.5$ m gained by k-ε model and the new zero-equation turbulence model using type A mesh. To show the detailed comparison of the results between k-ε model and the new zero-equation turbulence model, vertical profiles of the velocity are illustrated by Fig. 9. The testing points are chosen at the end of the recirculation zone, the two-third position in recirculation zone and the one-third position in the recirculation zone.

In type A mesh, the new zero-equation turbulence model's results agree reasonably well with the result of standard k-ε model. Both of the vertical and horizontal flow patterns show that the zero-equation turbulence model can reproduce the recirculation zone and the vortex behind the building as the k-ε model. Concerning the velocity data at a certain point, vertical profile show that zero-equation turbulence model can give results that are significantly consistent to the k-ε model. It can be concluded that under the best mesh the zero-equation model can perfectly take the place of k-ε model.

Fig. 10 shows the result of the simulation with type B mesh. In the coarser mesh type B, the recirculation beside the building

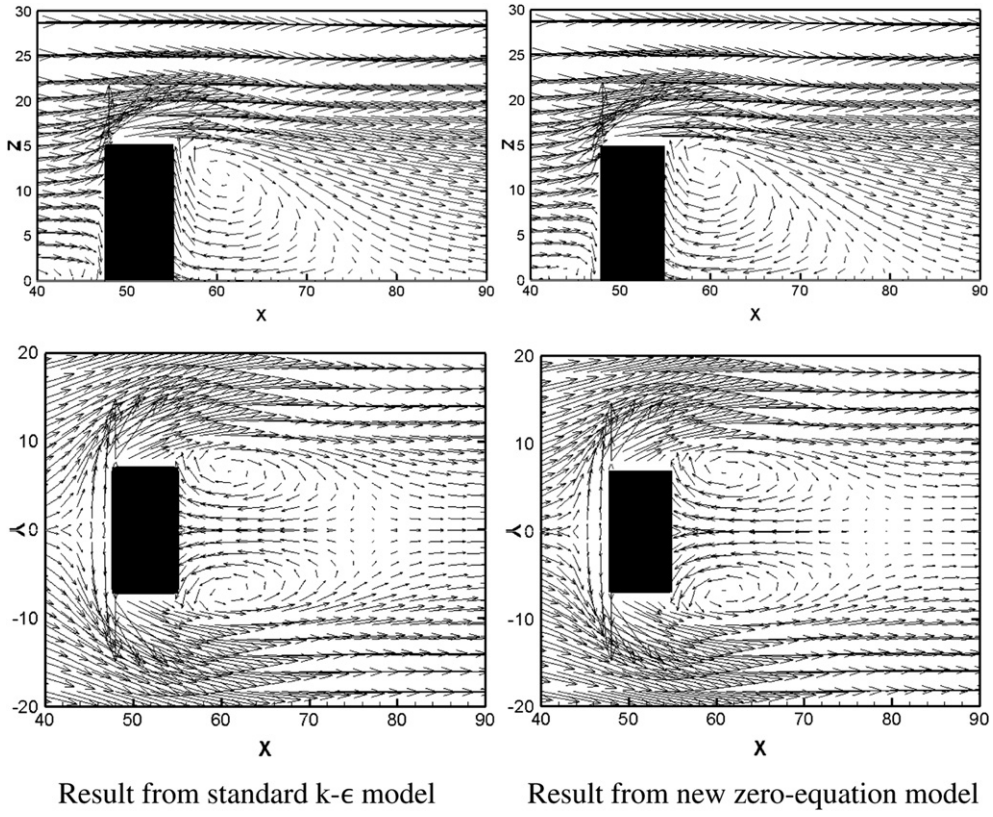

Fig. 10. Vertical profile and horizontal cross section at the height $z = 1.5$ m using type B mesh.

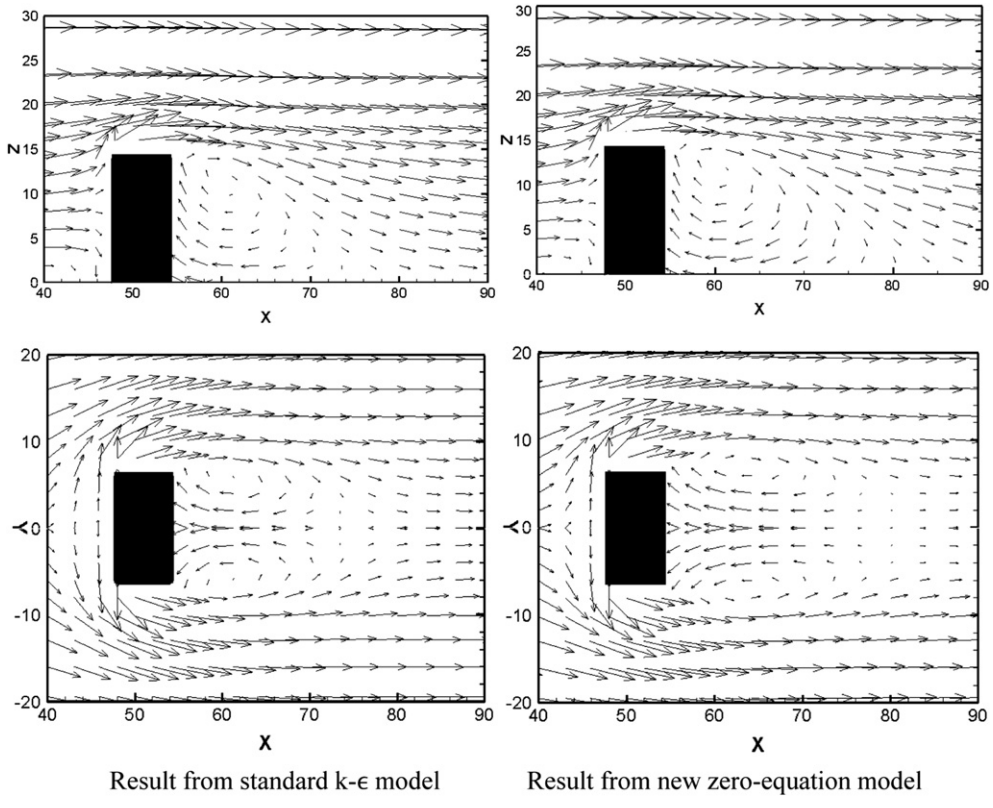

Fig. 11. Vertical profile and horizontal cross section at the height $z = 1.5$ m using type C mesh.

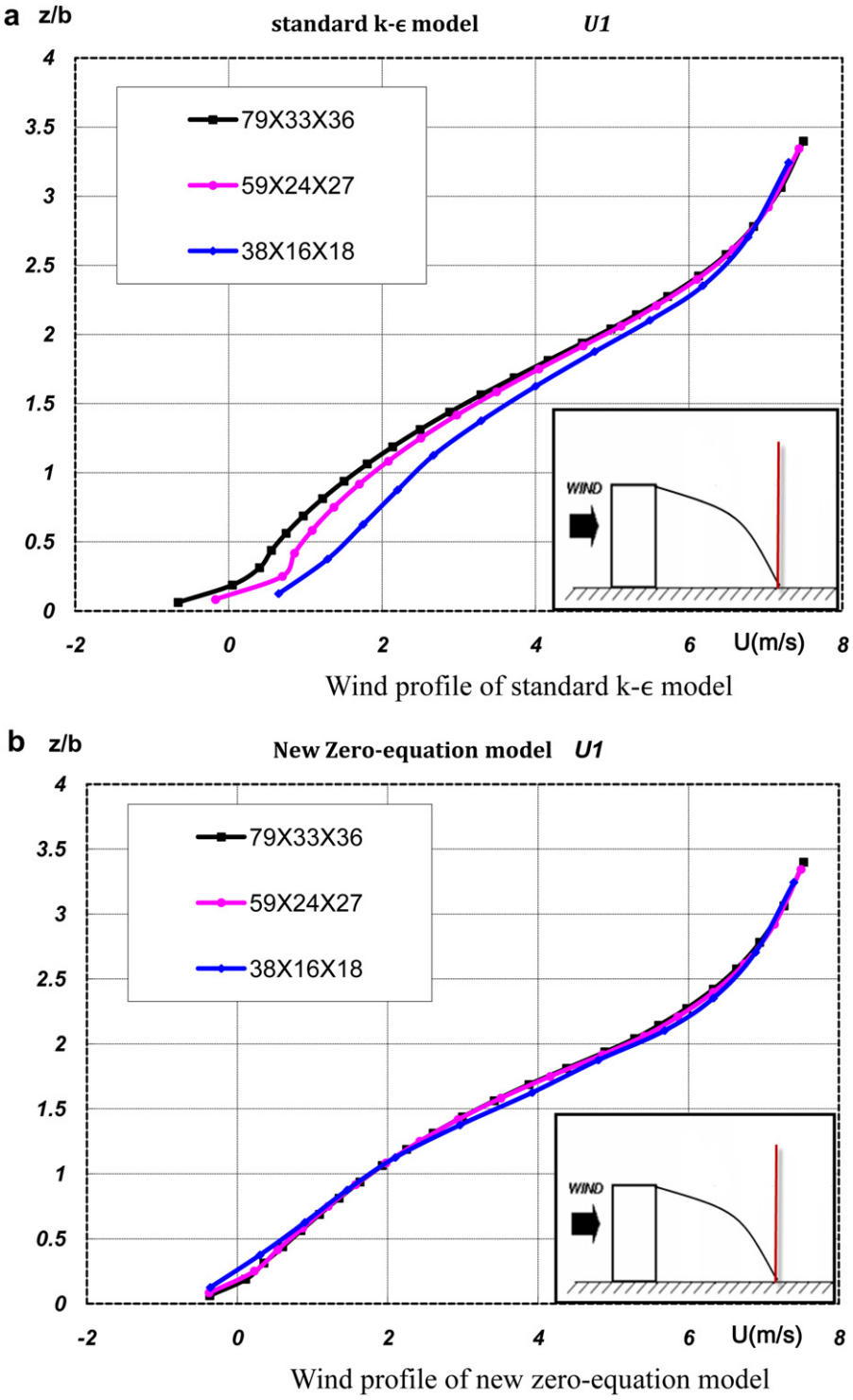

Fig. 12. Cross comparison of wind profile at the end of the recirculation zone.

disappeared, but the vortex behind the building can still be observed. Fig. 11 shows the result of the simulation with type C mesh. In the coarsest mesh type C, the size of the recirculation zones given by standard k-ε model and the zero-equation model decreases.

The cross comparison of all the mesh settings is conducted in order to test the influence made by the mesh resolution on each turbulence model. Position of testing point is chosen at the end of the recirculation zone.

Fig. 12(a) shows that different mesh settings will significantly influence the simulation results while using the standard k-ε model which has already been a consensus in the CFD field. Fig. 12(b) illustrates that the new zero-equation turbulence model is more robust than the k-ε model. This phenomenon indicates that coarse mesh setting could still be applied on the new zero-equation model, which can improve the computational efficiency in addition to reducing differential equations to be solved. Moreover, a CPU time test is also conducted to compare the simulation time

Table 2
comparison of the computer performance of the zero-equation model and the k-ε model.

NUM.	Mesh settings	Turbulence model	Computational time (sec)
1	79 × 33 × 36	Standard k-ε	1500
		New zero-equation	470
2	59 × 24 × 27	Standard k-ε	406
		New zero-equation	152
3	38 × 16 × 18	Standard k-ε	50
		New zero-equation	21

taken by the two models. Computational time is calculated by the code of simulation itself. According to Table 2, it is clear that the zero-equation turbulence model can save the CPU time and increase the efficiency of simulation to some extent.

6. Application on multi-building simulation

To test the performance of zero-equation turbulence model in multi-building condition, simulations are conducted by using both standard k-ε model and the new zero-equation turbulence model.

The nine buildings in simulation are all 8 m × 8 m × 16 m with the interval of 12 m between each other. Boundary conditions and numerical settings are the same as the single-building case. Comparison indicates the new zero-equation turbulence model can give similar flow patterns as the k-ε model (Fig. 13). Concerning the recirculation behind the building, vortexes behind all the three rows are similar in zero-equation and k-ε cases (Fig. 13). At the area behind buildings vortexes could be represented properly. Meanwhile, Fig. 14 shows the value of velocity at different testing points. According to Fig. 14 zero-equation model causes some deviation when the velocity is relatively low between two columns of buildings, but in general the zero-equation model agrees well with the standard k-ε model.

7. Discussion and conclusions

To reduce the computer load and increase the efficiency in micro-scale climate simulation, this paper proposes a new zero-equation turbulence model. This new zero-equation turbulence model is in the form of a two-layer model. In the inner layer the turbulence viscosity is a function of length scale and velocity deformation rate. In the outer layer the turbulence viscosity is expressed as a function of local mean velocity and length scale.

Comparison between the wind-tunnel experiment data and the simulation results obtained by the new zero-equation model shows that the results of simulation can agree well with the experiment data. The new zero-equation model exhibits the same ability to capture recirculation as standard k-ε model in validation case. The reattachment length given by zero-equation model is 2.38b while k-ε model gives 2.5b in the same case.

Further case studies analyze the capacity of the new zero-equation turbulence model by using it in single-building and multi-buildings applications. The simulation results are compared with those of standard k-ε model and comparison showed that the new zero-equation turbulence model can get reasonably acceptable results in practice application. The capability to capture recirculation in real size simulation is also reliable. Meanwhile, sensitivity analysis shows that the new zero-equation model is more robust on coarse mesh configuration so that it can efficiently decrease the computer load and speed up the simulation by using coarse mesh.

According to the validation and the application cases discussed above, in which Reynolds number are 10^4 and 1.31×10^7 respectively, the new zero-equation model shows similar performance as k-ε model when dealing with high Reynolds number simulation. Since the parameter in the zero-equation model is calibrated based on the high Reynolds number simulation using k-ε model, it could be concluded that this model is a suitable substitute for k-ε model in high Reynolds numbers situations.

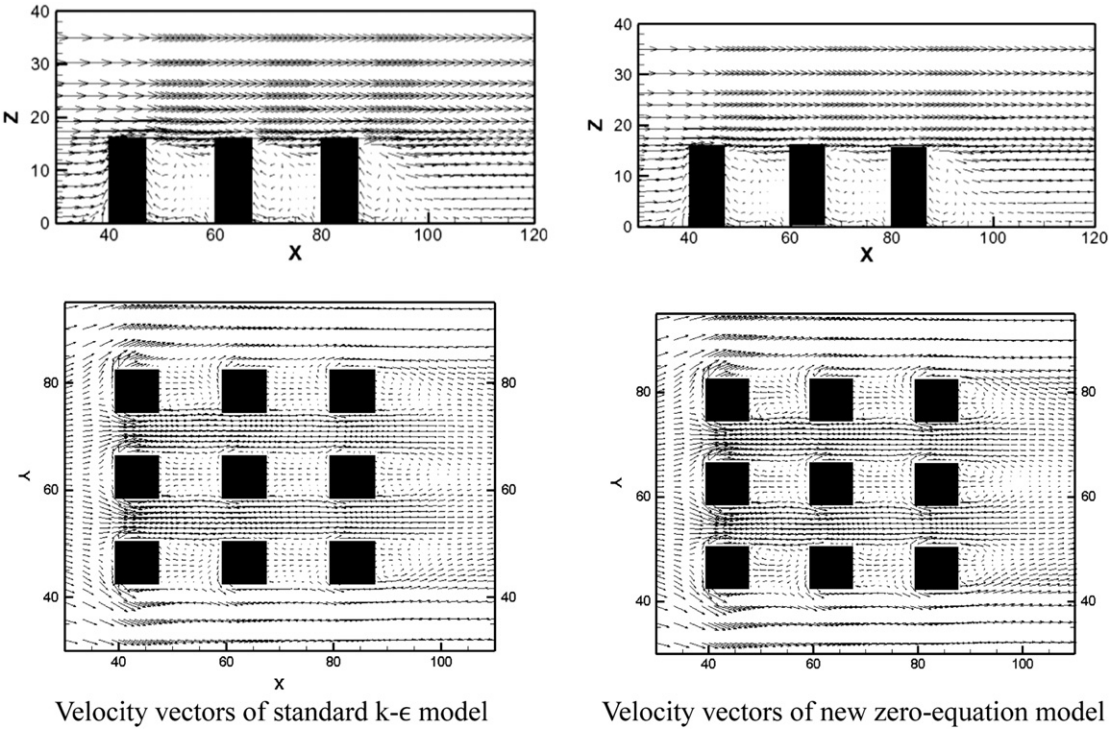

Fig. 13. Vertical profile and horizontal cross section at the height $z = 1.5$ m.

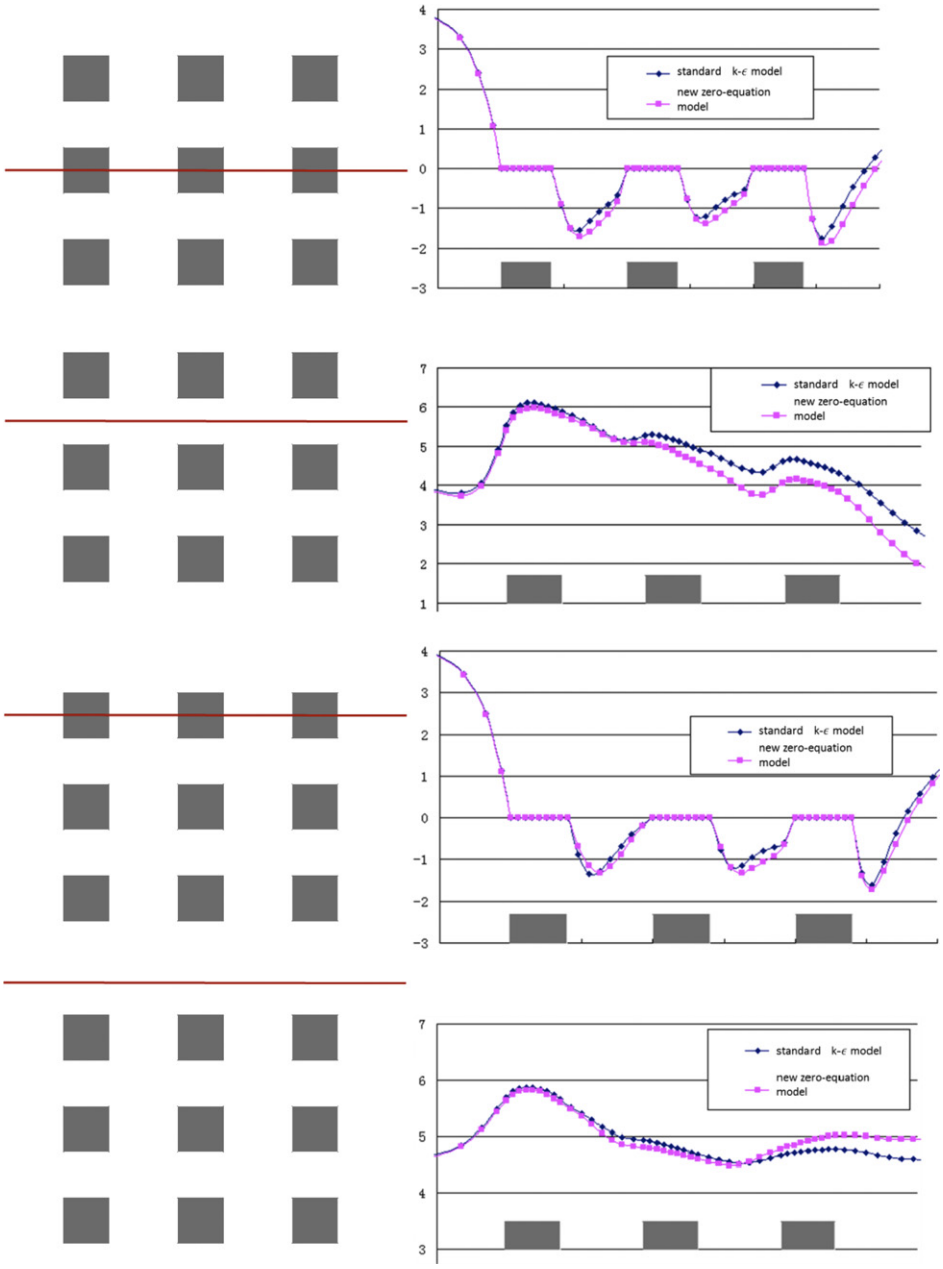

Fig. 14. Vertical profile at testing points.

Besides, all the simulations discussed in this paper are all isothermal cases. However, airflow driven by thermal buoyancy which is an important type of airflow in micro-climate is not considered. Therefore, further research would be conducted in a coupled thermal environment simulation platform considering buoyancy effect in order to analyze the performance in thermal driven airflow simulation.

References

[1] Mochida A, Lun IYF. Prediction of wind environment and thermal comfort at pedestrian level in urban area. J Wind Eng Ind Aerod 2008;96:1498–527.
[2] Murakami S, Mochida A, Ooka R, Yoshida S, Yoshino H, Sasaki K. Evaluation of the impacts of urban tree planting in Tokyo based on heat balance model. 11th international conference on wind engineering, Texas, USA 2003.
[3] Chen H, Ooka R, Kato S. Study on optimum design method for pleasant outdoor thermal environment using genetic algorithms (GA) and coupled simulation of convection, radiation and conduction. Build Environ 2008;43:18–30.
[4] Ooka R, Harayama K, Murakami S, Kondo H. Study on urban heat islands in Tokyo metropolitan area using a meteorological mesoscale model incorporating an urban canopy model. Fifth symposium on the urban environment. Vancouver 2004.
[5] Chen H, Ooka R. Study on energy efficiency and improvement of outdoor thermal environment with introducing distributed local energy supply systems in a densely built-up area in Tokyo. International symposium on sustainable development of Asia city environment (SDACE 2005); 2005.
[6] Chen H, Ooka R, Huang H, Nakashima M. Study on the impact of sensible heat flux from building walls and artificial heat release from buildings on outdoor thermal environments using coupled simulations of convection, radiation, and conduction. The sixth international conference on urban climate (ICUC6); 2006.
[7] Murakami S. Indoor/outdoor climate design by CFD based on the software platform. Int J Heat Fluid Flow 2004;25:849–63.
[8] Li X-X, Liu C-H, Leung DYC, Lam KM. Recent progress in CFD modelling of wind field and pollutant transport in street canyons. Atmos Environ 2006;40:5640–58.
[9] Tominaga Y, Mochida A, Yoshie R, Kataoka H, Nozu T, Yoshikawa M, et al. AIJ guidelines for practical applications of CFD to pedestrian wind environment around buildings. J Wind Eng Ind Aerod 2008;96:1749–61.
[10] Yoshie R, Mochida A, Tominaga Y, Kataoka H, Harimoto K, Nozu T, et al. Cooperative project for CFD prediction of pedestrian wind environment in the Architectural Institute of Japan. J Wind Eng Ind Aerod 2007;95:1551–78.

[11] Mirzaei PA, Haghighat F. Approaches to study urban heat island - abilities and limitations. Build Environ 2010;45:2192–201.
[12] Xie X, Liu C-H, Leung DYC. Impact of building facades and ground heating on wind flow and pollutant transport in street canyons. Atmos Environ 2007;41:9030–49.
[13] Chen H, Ooka R, Harayama K, Kato S, Li X. Study on outdoor thermal environment of apartment block in Shenzhen, China with coupled simulation of convection, radiation and conduction. Energ Build 2004;36:1247–58.
[14] Chen Q, Xu W. A zero-equation turbulence model for indoor airflow simulation. Energ Build 1998;28:137–44.
[15] Srebric J, Chen Q, Glicksman LR. Validation of a zero-equation turbulence model for complex indoor airflow simulation. ASHRAE Trans 1999;105: 414–27. Part2.
[16] Zhai Z, Chen Q, Haves P, Klems JH. On approaches to couple energy simulation and computational fluid dynamics programs. Build Environ 2002;37:857–64.
[17] Zhai Z, Chen Q. Solution characters of iterative coupling between energy simulation and CFD programs. Energ Build 2003;5:493–505.
[18] Zhai Z, Chen Q. Performance of coupled building energy and CFD simulations. Energ Build 2005;37:333–44.
[19] Prandtl L. Uber die ausgebildete. ZAMM 1925;5:136–9.
[20] Prandtl L. Fürher durch die Strömungslehre. Braunschweigh Vieweg und Sohn; 1942. p. 407.
[21] Cebeci T, Smith AMO. Analysis of turbulence boundary layers, series in applied mathematics and methods: XV. Academic Press; 1974.
[22] Baldwin BS, Lomax H. Thin-layer approximation and algebraic models for separated turbulence flows AIAA paper. Huntsville, AL; 1978. 78–257.
[23] Liu H, Ikehata M. Computation of free surface waves around an arbitrary body by a Navier-stokes solver using the psuedo compressibility technique. Int J Numer Meth Fluid 1994;19:395–413.
[24] Wilcox DC. Turbulence modeling for CFD, DCW industries; 1993. p. 51.
[25] FLUENT. Fluent 6.2 user's guide. Lebanon, NH: Fluent Inc.; 2005.
[26] Meng Y, Hibi K. Turbulent measurements of the flow field around a high-rise building. J Wind Eng Jpn 1998;76:55–64.
[27] Tominaga Y, Mochida A, Shirasawa T, Yoshie R, Kataoka H, Harimoto K, et al. Cross comparisons of CFD results of wind environment at pedestrian level around a high-rise building and within a building complex. J Asian Architect Build Eng 2004;3:63–70.